Highly Fluorescent Conjugated Polyelectrolyte Nanostructures: Synthesis, Self-Assembly, and Al^{3+} Ion Sensing

*Jungmok You, Jeonghun Kim, Teahoon Park, Byeonggwan Kim, and Eunkyoung Kim**

A highly fluorescent triazine-bridged polymer, poly[(diphenylamino-s-triazine)-co-(2-methoxy-5-propyloxysulfonate-1,4-phenylene vinylene)] (DTMSPV), is synthesized from Wittig polycondensation of a triazine monomer with a water-soluble *p*-phenylene vinylene monomer. The fluorescent amphiphilic polymer in aqueous solution self-assembled into nanoassemblies of micelle-like nanostructure (MS) and π stacking nanostructure (πS), which have average sizes of 93 to 270 nm, depending on the concentration of DTMSPV. The micelle-like nanostructure of DTMSPV (MS) shows blue emission at 457 and 488 nm with a high emission quantum yield (Φ_E) of 31% in aqueous solution. On the other hand, the Φ_E of π stacking structures (πS), formed in a highly concentrated solution, is lower than the MS. The MS exhibits fluorescence quenching as well as color change from blue to green/yellow, depending on the kinds of metal ions. The metal ion sensitivity is larger in the order of the main group ions (Na^+, K^+) < dicationic transition metal ions (Zn^{2+}, Cd^{2+}, Pb^{2+}, Cu^{2+}, Pd^{2+}) < trivalent transition metal ions (Fe^{3+}, Ru^{3+}), with an exception of Al^{3+}. In particular, the fluorescence of MS is dramatically quenched with color change to yellow in response to Al^{3+} concentrations. The selectivity and sensitivity of MS to Al^{3+} are unusually high even in the presence of competitive metal ions, which can be attributed to the specific interaction of triazine units with Al^{3+}.

1. Introduction

Various advanced materials in nanospaces or nanostructures are of great interest in sensing and removal of environmentally deleterious substances.[1] Among them, fluorescent nanomaterials such as colloidal nanoparticles (quantum dots),[2] dye doped silica,[3] gold nanoparticle-fluorescent polymer complex,[4] and polymer particles[5] are an attractive materials which have proven to be versatile and powerful sensing properties with unique optical properties. The high sensitivity of fluorescent nanostructures (NSs) is originated from the large number of both binding sites and fluorophores.[6] The inherent large surface area in NSs provides more than the necessary binding sites at the fluorescent nanostructure surfaces, which allow efficient interaction with the target ions or molecules, to result in high binding efficiency.[5]

Among the materials for fluorescent nanostructures, polymers derived from conjugated organic molecules have been used in the application for sensing and imaging. The physical properties of fluorescent polymer nanostructures are comparable to the well known alternatives, such as quantum dots, dye-doped silica, and self assembled organic dye crystals.[7] However fluorescent polymer nanostructures are relatively benign and appear to be promising for uses in environment and imaging studies where the toxicity of nanostructures may be a concern. Furthermore, color tuning of the polymer is easily achieved by changing the monomer structure and degree of polymerization. As the fluorescent dye molecules are covalently bound in polymer, the stability of these polymer nanostructures in biological media is expected much longer than the dye doped system or dye crystals which suffer diffusion and dissolution of dye molecules into the media over time.

In particular, fluorescent polyelectrolytes, widely used for biosensors and metal ion sensors, are challenging as they can be readily processed to nanoscaled structures by self assembly arising from their amphiphilic characteristics.[8] Nonetheless, self-assembled fluorescent nanostructures of polyelectrolyte have been much less explored relative to a number of reports on fluorescent dye-doped nanoparticles and quantum dots. One of the shortcomings in fluorescent polyelectrolytes is their poor selectivity which is originated from nonspecific electrostatic interactions between conjugated polyelectrolyte and complementarily charged quencher.[9] Moreover low fluorescence quantum yields of polyelectrolytes have limited their application toward optical detection.

To synthesize highly fluorescent polyelectrolyte bearing metal selectivity, it is a challenge to modify a polyelectrolyte backbone with metal binding units such as nitrogen ligands and ionic group plus a well-ordered fluorescent unit of conjugated polymer chain. The ionic groups such as sulfonate groups

J. You, J. Kim, T. Park, B. Kim, Prof. E. Kim
Active Polymer Center for Pattern Integration
Department of Chemical and Biomolecular Engineering
Yonsei University
50 Yonsei-ro, Seodaemun-gu
Seoul 120-749, South Korea
E-mail: eunkim@yonsei.kr

DOI: 10.1002/adfm.201102309

provide not only water solubility but also metal sensing sites through electrostatic interaction with cations.[10] On the other hands, multidentate nitrogen ligands possess high binding affinities for metal ions due to a chelation effect. For example, triazine-containing molecules can be used as specific intercalating ligands for several metals such as ruthenium (III),[11] zinc(II),[12] and copper(II).[13] Moreover, a molecular dynamics simulation revealed that a triazine unit could interact favorably with Al(III).[14] Thus, triazine was selected as a metal binding unit and designed to couple with a *p*-phenylene vinylene (PPV) unit, according to the previous method for the synthesis of a highly fluorescent polymer.[15]

Amphiphilic conjugated polyelectrolytes, which is consist of rigid-rod polymer backbones and ionic side groups, easily aggregate into nanostrutures in aqueous solution as well as even in good solvent through self-assembly.[16,17] Taking advantage of such aggregation, we have synthesized highly fluorescent amphiphilic polyelectrolytes, which could form NSs even in the absence of surfactants. Herein we report a unique approach to constructing new nanostructures of fluorescent polymer, composed of repeating binding sites of triazine units and sulfonate side groups. To the best of our knowledge, this report contains the first example of highly fluorescent polymer nanoassemblies with dual-metal binding sites.

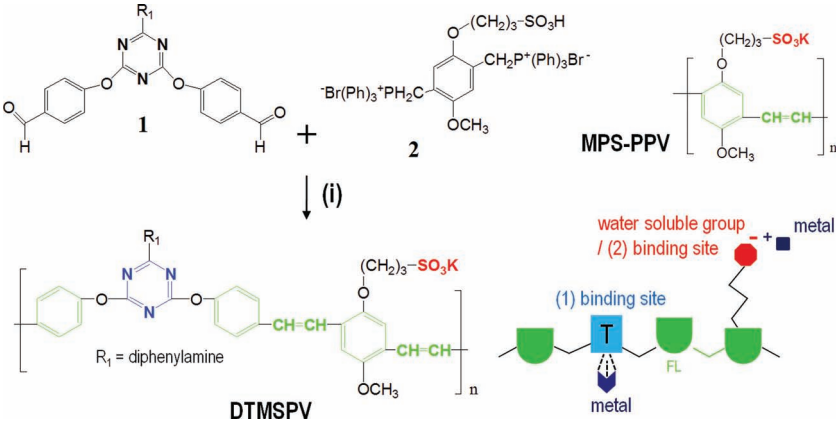

Figure 1. The synthesis of the DTMSPV polymer. (i) t-BuOK, DMF, THF, tert-butanol, at 40 °C. The schematic illustration of DTMSPV and chemical structure of MPS-PPV.

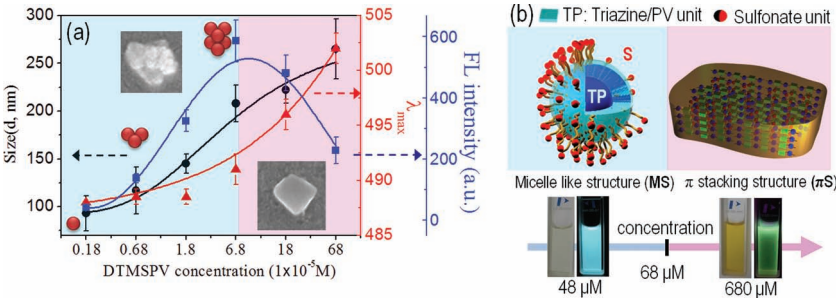

Figure 2. a) DTMSPV concentration dependence of nanostructure size, emission maxima (λ_{max}), and emission intensity. λ_{exc} = 370 nm. b) Schematic illustration of DTMSPV nanostructure depending on DTMSPV concentration. Photographic images of DTOMPV in the aqueous solution (4.8×10^{-5} M and 6.8×10^{-4} M) under the room light and excited at 365 nm using a hand-held UV lamp.

2. Results and Discussion

2.1. Synthesis and Optical Properties of Fluorescent Polymer Nanostructures

Triazine bridged amphiphilic polymer was synthesized by Wittig polycondensation reaction with a triazine (**1**) and a water-soluble 1,4-phenylene vinylene (**2**), as illustrated in **Figure 1**. The FT–IR spectrum of DTMSPV (Figure S1b, Supporting Information) showed vibration peaks at 865 cm^{-1} and 1600 cm^{-1}, characteristic of the C=C vinylene of the polymer backbone and the C=N stretching peak of the triazine unit,[18] respectively. The spectral data for the sulfonated *p*-phenyene vinylene units were compared with those of the poly(2-methoxy-5-propyloxy sulfonate, 1,4-phenylene vinylene (MPS-PPV as show in Figure 1), homopolymer without triazine unit (Figure S1a, Supporting Information). The average molecular weight of the polymer was estimated by ^{1}H-NMR as 13,200 as described in the Experimental Section. Thus DTMSPV consists of three different functional units: triazine and sulfonate unit for metal interaction, *p*-phenylenevinylene for fluorescence, and a sulfonate unit to confer water solubility (Figure 1).

The amphiphilic DTMPSV was self assembled into nanostructures having average sizes of 93 to 270 nm as determined by a dynamic light scattering technique (DLS) (**Figure 2**a, black line). Of our surprise, the structures of the nanoassemblies were various depending on the concentration as clearly confirmed via electron microscopes of FE-SEM and HR-TEM (**Figure 3**). When the DTMSPV concentration was low (0.18~6.8×10^{-5} M), the nanoassemblies were appeared as micelle like structures (MSs) with average size of 93~210 nm, which were consist of small nanoparticles (30~40 nm). In these aggregated forms, the hydrophobic DTMSPV backbones, consisting of triazine (**T**) and *p*-phenylene vinylene (**P**), could be located inside and surrounded by the hydrophilic sulfonate (**S**) side chains (Figure 2b). This is probably due to rigid polymer backbone composed of phenylene and triazine unit. DTMSPV MSs were clearly observed even in very dilute solution (1.8×10^{-6} M) but a far less amount. These micelle like structures have been described previously for an amphiphilic compounds.[8b–d] Such a concentration dependent aggregation of polymeric particles into larger aggregations are due to the amphiphilicity of the polymer as often found from the functional polymers.[19] The stability of DTMSPV MSs dispersed in aqueous solution was investigated by the zeta potential measurements. The zeta potential was determined as –46.1 mV, which indicates

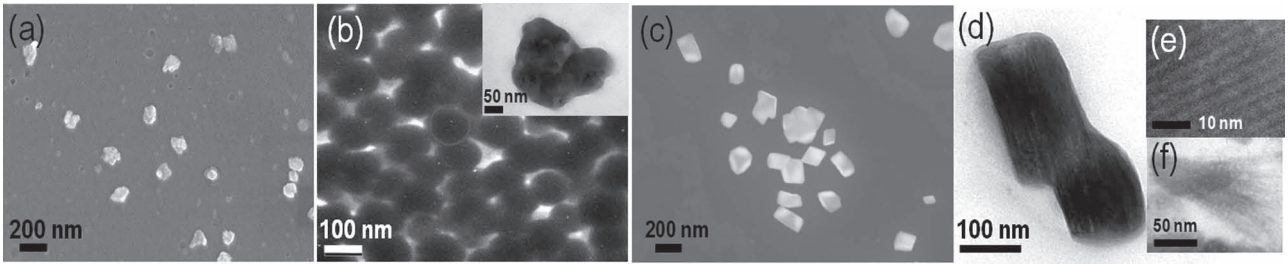

Figure 3. a) and b) SEM and TEM images of DTMSPV micelle like structures (DTMSPV-MS) in aqueous solution (6.8×10^{-5} M), respectively. b) Inset: Cross-sectional TEM image of DTMSPV-MS. c) and d) SEM and TEM images of DTMSPV π-stacking structure (DTMSPV-πS) in aqueous solution (6.8×10^{-4} M). e) Magnified TME image of DTMSPV-πS. f) Cross-sectional TEM image of DTMSPV-πS.

good stability of the micelle like structures probably derived from the anionic sulfonate groups stretched out.

When the DTMSPV concentration was further increased to 6.8×10^{-4} M, the average particle size of nanostructures was increased up to 270 nm and the structure was changed to plates as depicted in Figure 2. The SEM and TEM image clearly shows the plate structures comprising bundle of hairy structures having interpolymer π stacking aggregations (π**S**) as shown in Figure 3c and d. The polymer basically consists of aromatic main chain (**TP**) and flexible polar propylene sulfonates (**S**). Thus the π stacking aggregations could be described as self-assembly of the TP (aromatic main chain) rod separated by the sulfonates. The aromatic mainchain was appeared as black strip due to the staining in the TEM image[31] and thus the π stacking distance could be approximately estimated as within 1.2 ~ 1.5 nm from Figure 3e. The interpolymer distance for the co-facially arranged phenylene rings on adjacent polymer backbone was reported as within 3.6 ~ 4.3 Å.[20] Therefore, the co-facially arranged polymer backbone of aromatic mainchain and interpolymer distance were totally calculated as within 1.2 ~ 1.3 nm (Figure S2, Supporting Information), which was matched to Figure 3e.

The cross-sectional TEM image in Figure 3f shows also the π stacking arrangements of the polymer mainchain, which originated from the planar conformation of aromatic units. Compared to MSs, the πSs are much bigger with an average size of 260 nm and more edged types to form a cofacial planar structure.

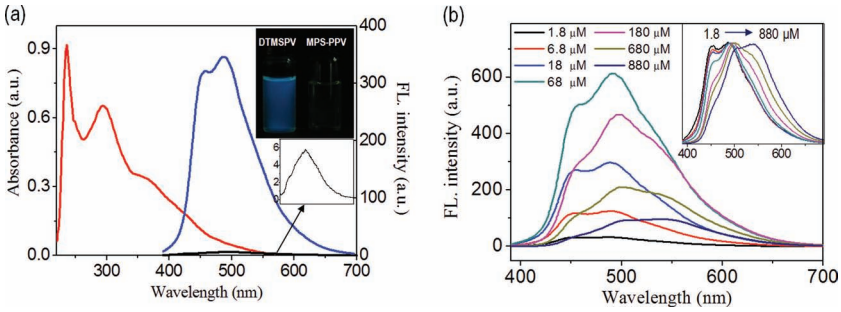

Figure 4. a) UV–vis absorption and fluorescence spectra of the DTMSPV in aqueous solution (4.6×10^{-5} M) at excited at 370 nm in comparison with the fluorescence spectrum of MPS-PPV in aqueous solution (black line) at excited at 370 nm. The inset shows magnified fluorescence spectra of MPS-PPV and photographic images of DTMSPV (left) and MPS-PPV (right) in aqueous solution with same concentrations (4.6×10^{-5} M) excited at 365 nm. b) Fluorescence spectra of the DTMSPV at different concentration and normalized spectra (inset) to show spectral shift.

2.2. Fluorescence Properties of MS and πS

The orange colored DTMSPV solids took pale yellow color when dissolved in water to show absorption bands maximized at 245, 300, and 360 nm (**Figure 4**a). The DTMSPV in aqueous solution exhibited blue fluorescence, showing two strong bands maximized at 457 and 488 nm with a shoulder at ~540 nm under an excitation probe at 370 nm (Figure 4a). The broad and long-wavelength absorption and emission spectra of DTMSPV in aqueous solution indicate that DTSMPV exist in an aggregated state.[21] The shape of the bands were similar to those of PPV derivatives which show two or three emission bands at around 450 ~ 630 nm.[22] Surprisingly, the absolute fluorescence quantum yield (Φ_{AE}) DTMSPV in water (8×10^{-6} M) was very high as 31%, unlike the water soluble PPV derivatives such as MPS-PPV, as determined from an integrating sphere. The quantum yield is much higher than the reported fluorescent polymers including the conjugated polymer, poly{2,5-bis[3-(N,N,N-triethylammonium bromide)-1-oxapropyl]-1,4-phenylenevinylene (14%), and 31-fold higher than that of MPS-PPV (<1%).[23] As compared in Figure 4(a, black line), the aqueous solution of MPS-PPV exhibited very weak fluorescence and its intensity was ~3% of the aqueous DTMSPV solution at the same concentration. This high Φ_{AE} for DTMSPV is probably due to the alternatively connected rigid units of triazine and phenylene, which likely increases the planarity along the polymer backbone to reduce self-quenching.[32]

Due to the self assembling character, the fluorescence maximum and intensity of DTMSPV nanostructures in aqueous media were highly sensitive to the concentration of DTMSPV. In a very dilute solution, the fluorescence was small with a maximum (λ_{max}) at 488 nm. In a more concentrated solution, the fluorescence intensity was stronger with increase in shoulder band beyond 540 nm as the concentration was higher. The λ_{max} was observed at 542 nm, however, the intensity was dramatically decreased in a highly concentrated solution (8.8×10^{-4} M,

Figure 4b). The fluorescence band shift and intensity increase were correlated to the size of DTMSPV nanostructure up to the concentration of 6.8×10^{-5} M as shown in Figure 2a (red and blue lines). The fluorescence intensity of the 6.8×10^{-5} M solution was 6 times higher than the dilute solution (1.8×10^{-6} M), however, it was decreased sharply when the concentration was higher than 6.8×10^{-5} M, although band was further shifted to red. The spectral shift and intensity increase in the concentration rage at 1.8×10^{-6} M ~ 6.8×10^{-5} M could be understood considering the fact that DTMSPV nanostructures form micelle like particles. In the micelle like structures, the sequential red shifted fluorescence maxima with the increase in size indicate a decrease in the bandgap, arising from the increase in effective conjugation length.[24] As the agglomeration among the small particles are enhanced in a higher concentration, the DTMSPV chains could be more squeezed and confined in a small MS, to increase fluorescence intensity.

The changes of both spectral shift and fluorescence quenching in a high concentration (above 6.8×10^{-5} M) are characteristic for the formation of interpolymer π stacking aggregations (πS),[8a,25] as evidently shown in Figure 2 and 3. As shown in the simulated structures (Figure S2, Supporting Information), this π stacking leads the phenylene rings to adopt an all-planar conformation to allow stronger interactions between the aromatic rings, which eventually lead fluorescence quenching. Since the fluorescence of the DTMSPV is sensitive to surrounding environment such as concentration and solvent, we extend our study toward metal ion sensing, using the most fluorescent DTMSPV MS solution (6.8×10^{-5} M).

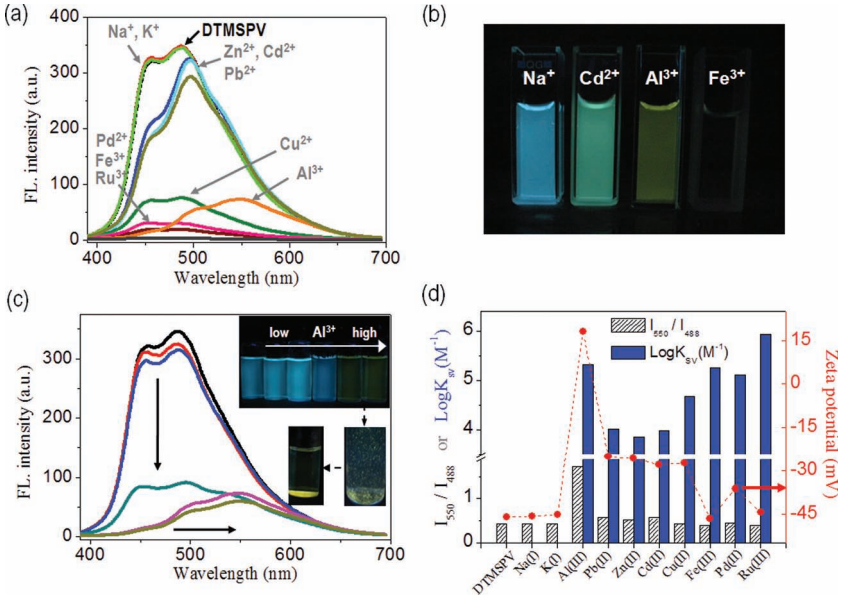

Figure 5. a) Emission spectra of DTMSPV solution (4.6×10^{-5}M) and on addition of metals of Na^+, K^+, Zn^{2+}, Cd^{2+}, Pb^{2+}, Cu^{2+}, Pd^{2+}, Fe^{3+}, Ru^{3+}, and Al^{3+} (7.2×10^{-5}M) in aqueous solution. λ_{exc} = 370 nm. b) Photographic images of DTMSPV in aqueous solution after the addition of Na^+, Cd^{2+}, Al^{3+}, and Fe^{3+} excited at 365 nm using a hand-held UV lamp. Metal concentration is 7.2×10^{-5}M. c) Emission spectra of DTMSPV (4.6×10^{-5}M) in aqueous solution depending on $AlCl_3$ concentration. (From top to bottom: 0, 3.6, 12, 36, 72, and 360 μM.) d) Stern-volmer constant (K_{sv}), emission intensity ratio (I_{550}/I_{488}), and zeta potential change of DTMSPV for metal ions.

2.3. Detection of Metal Ions

The blue fluorescence from DTMSPV-MSs remained almost intact in the presence of group I ions such as Na^+ and K^+. However, it changed dramatically in the presence of divalent and trivalent ions as shown in **Figure 5**a. The fluorescence quenching by metal ions were wavelength selective, allowing us to determine the sensitivity of DTMSPV for each metal ions (Figure S3, Supporting Information). When divalent transition metal ions (group II) such as Zn^{2+}, Cd^{2+}, or Pb^{2+} was present, fluorescence quenching at 457 nm (v_{00}) was larger than that at 488 nm (v_{01}) to change the color of fluorescence from blue to green (Figure 5b). The quenching was more efficient with Cu^{2+} and Pd^{2+}, resulting in the fluorescence quenching at both 457 nm and 488 nm. The fluorescence of DTMSPV was completely quenched by Fe^{3+} and Ru^{3+}, leaving only trace of fluorescence at both bands. Interestingly, when Al^{3+}, one of the post transition metals, was present, there was large fluorescence quenching both at 457 nm and 488 nm; however, the fluorescence band at 550 nm (v_{02}) was increased to some extent, resulting in a color change of emission from blue to yellow green (Figure 5c). The effect of metal ions on fluorescence color change of DTMSPV-MSs was evident to the naked eye as shown in Figure 5b, which clearly shows the intact blue, green, yellow green fluorescence, and complete fluorescence quenching of DTMSPV-MSs in aqueous solution after the addition of Na^+ (group I), Cd^{2+}(group II), Al^{3+}, and Fe^{3+} (group III), respectively.

Stern-Volmer plots for the fluorescence quenching of DTMSPV-MSs showed a linear relationship between fluorescence intensity ratio (I_o/I) and metal ion concentration (Figure S4, Supporting Information), where I_o and I are the fluorescence intensity of the solution in the absence and presence of metal ions, respectively. Based on the slopes of the plots, the Stern-Volmer quenching constants (K_{sv}), which is used as a good estimate for the binding constant of complex formation,[26] were determined as listed in Table S1 (Supporting Information) and Figure 5(d, blue bar). The K_{sv} in the presence of trivalent Ru^{3+}, Al^{3+}, and Fe^{3+} among the largest as 879400, 209300, and 182700 M^{-1}, respectively, revealing that Ru^{3+} is the most sensitive ion to DTMSPV. Al^{3+} was the 2nd most sensitive ion among the metal ions. Importantly, the K_{sv} of DTMSPV with Al^{3+} was ~100 time larger than that of the MPS-PPV without triazine unit (2590 M^{-1}).[27] This result clearly indicates that DTMSPV exhibits unusually high sensitivity to Al^{3+}, possibly originated from the triazine units, which are present in DTMSPV not in MPS-PPV.

2.4. Al^{3+} Ion-Specific Aggregation of DTMSPV-MSs

Addition to the high sensitivity to Al^{3+}, the fluorescence spectral change of DTMSPV-MSs with Al^{3+} is characterized as

quenching plus spectral shift, while it is quenching only over whole spectral region with the other metal ions. Such a unique spectral behavior of DTMSPV provided an exclusive method for Al^{3+} sensing. As shown in Figure 5d (black bar), Al^{3+} was non-comparable to other metal ions when monitored the fluorescence intensity change at 550 nm against 488 nm. Because the spectral changes of DTMSPV-MSs in the presence of Al^{3+} were distinguishable from other metal ions, we evaluated the selectivity of DTMSPV for Al^{3+} by examining the ratio (S_l) of the emission intensity at 550 nm and 488 nm ($S_l = I_{550}/I_{488}$) of the DTMSPV solution containing Al^{3+} in the presence of other metal ions (Figure S5, Supporting Information). DTMSPV without Al^{3+} showed the lowest S_l value of 0.44 while DTMSPV with Al^{3+} exhibited the S_l value of 1.73 (Figure 5d). The S_l was kept above 1 by additional metal ions, indicating that DTMSPV can be used to detect Al^{3+} in the presence of competitive metal ions (Figure S5d and Table S1, Supporting Information). It decreased significantly to 0.52 by the addition of Ru^{+3}, which is the strongest quencher in this series of work. The S_l of DTMSPV in the presence of Pd^{+2} was relatively low, but Al^{3+} was still clearly detectable because of the change in the major emission bands (Figure S5b, Supporting Information). Figure S5c (Supporting Information) shows the detectable fluorescence change from blue to yellow in Al^{3+} solution in the presence of additional metal ions. Overall, our results indicate that DTMSPV is a highly selective sensing material for Al^{3+} in the presence of most competitive metals, with the exception of Ru^{3+}.

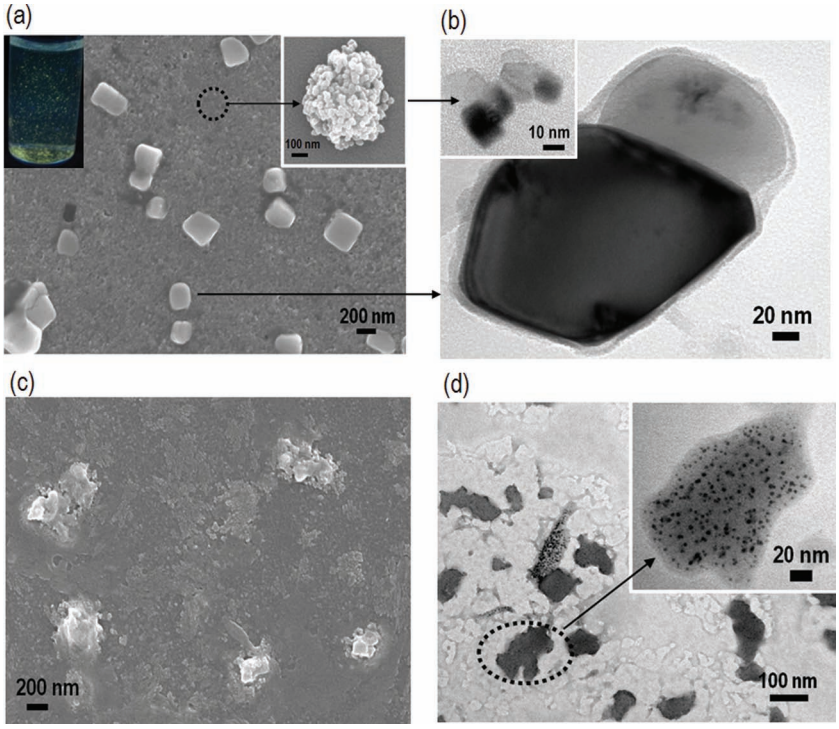

Figure 6. a) and b) SEM and TEM images of DTMSPV-MSs with a size of 194 nm in the presence of Al^{3+}. a) Inset: Photographic image of DTMSPV-MSs in aqueous solution after the addition of Al^{3+} (left) and magnified SEM images of small aggregated particles (right). b) Inset: TEM images of small aggregated particles. c) and d) SEM and TEM images of DTMSPV-MSs with a size of 194 nm in the presence of Cd^{2+}. d) Inset: Magnified TEM image of DTMSPV-MSs and Cd^{2+} complex. Metal concentration is 7.2×10^{-5} M.

The specific interaction of the DTMSPV-MSs with Al^{3+} was accompanied with red shifted absorption with enhanced long tail, which is characteristic of tightly aggregated forms. On the other hands there was no shift in absorption in the solutions containing other metals such as Cd^{2+} and Cu^{2+} (Figure S6, Supporting Information). Interestingly, the DTMSPV aggregation by Al^{3+} was accompanied by the formation of yellow fluorescent precipitates. When the Al^{3+} concentration was increased from 3.6 μM to 12 μM, the first and second band (max. at 457 and 488 nm, respectively) decreased. When the Al^{3+} concentration was increased further (≥72 μM), the emission was quenched and yellow solids were precipitated as shown in Figure 5c. On the other hands, the MPS-PPV solution did not afford yellow precipitation even when the MPS-PPV and Al^{3+} concentrations were very high as 100 μM and 360 μM, respectively. Also, any yellow precipitation was not shown in the DTMSPV solution by other metals, even a very high concentration (360 μM). Therefore, we could easily monitor the interaction of DTMSPV-MSs with Al^{3+} with even naked eye. Moreover these precipitations ensure an easy process for the removal of toxic Al^{3+} from environmental sources such as water using centrifugation.

The FT-IR spectrum of the precipitates from DTMSPV solution with Al^{3+} showed that the triazine peak (C=N stretching) of DTMSPV at 1600 cm^{-1} was changed, while other regions remained intact (Figure S1c, Supporting Information) upon complexation of Al^{3+}, suggesting that triazine units are critical for sensing and ultimately Al^{3+} ion-specific aggregation. This judgment is also supported by the report that Al^{3+} ions interact with the trivalent triazine units.[14]

Al^{3+} ion-specific aggregation of DTMSPV-MSs was further identified from the SEM and TEM images (**Figure 6**a and b of the precipitates obtained from the solution of DTMSPV-MSs (av. 194 nm size) with Al^{3+}. The DTMSPV-MSs was changed to plates in the presence of Al^{3+} (Figure 6a and b). The nano plates of the Al^{3+} aggregation with DTMSPV were similar to the πS formed under high DTMSPV concentration. However, the entire plates were black without dark lines in HR-TEM image, indicating that the interpolymer π stacking aggregations are disturbed by Al^{3+} aggregation with DTMSPV. As Al^{3+} ions specifically interact with triazine units of the aromatic main chains, the self-assembled πSs among the polymers are destroyed.

DTMSPV complex with other metals were similar to the pristine MSs as shown in Figure 6c and d for Cd^{2+} complex. The TEM image shows Cd^{2+} bound to the surface group, sulfonate groups, in the DTMSPV-MSs surface, which separately exist as black dot shapes (Figure 6d). These results indicate that sulfonate groups in the surface of DTMSPV nanoparticles are mainly functioned as metal binding sites for group II metals.

2.5. The Interaction of Metal Ions with DTMSPV Nanosturtures (NSs)

There are two different metal binding sites in DTMSPV NSs: sulfonate (S) and triazine units (T). The zeta potential, determined as –46.1 mV, of pristine DTMSPV-MSs, was almost intact in the presence of undisruptive metal ions (Na^+ or K^+) (Figure 5d, red circle). In the presence of dications (Pb^{2+}, Zn^{2+}, Cd^{2+}, Cu^{2+}, and Pd^{2+}), the zeta potential was reduced to –36.2 and –27.5 mV. This indicates that the dicatons interact with sulfonate anions, possibly forming a bidentate complex. This result matched to the above microscopic results.

In the presence of trivalent ions such as Fe^{3+} and Ru^{3+}, zeta potential was almost similar as the pristine DTMSPV-MSs. Since the quenching of the fluorescence is obvious and very efficient, the zeta potential data indicates that these metal ions could be interacted with the triazine units located inside MSs, not sulfonate anions, keeping the zeta potential same as that of pristine. Due to the Al^{3+} specific aggregations and precipitation, Al^{3+} resulted in the largest change of zeta potential among the metals to show zeta potential of +18.0 mV (Figure 5d). From the zeta potential study, the metal ions could be categorized into two groups, triazine binding metals and sulfonate binding metals. This specific interaction of triazine with trivalent ions (Fe^{3+}, Ru^{3+}, and Al^{3+}) over other metal ions could be attributed to their small size as well as trivalent ionic nature (Table S1, Supporting Information), which allow the ions to penetrate easily into DTMSPV-MSs and interact effectively with the three nitrogen atoms in the triazine unit, respectively.

Since the triazine units are located more in the inner part, while the hydrophilic sulfonate groups are more on the surface, the fluorescence quenching by Al^{3+} and Ru^{3+} was highly dependent on the size and shape of DTMSPV-NSs. As the size of DTMPSV-NSs was increased, the opportunity of interaction between triazine and these metals were significantly decreased due to the location of triazine unit packing up inside DTMSPV-NSs. Thus the small size DTMSPV-NSs (106 and 149 nm) were much sensitive to Al^{3+} ions than those with large size DTMSPV-NSs (194 and 233 nm) in a high Al^{3+} concentration (Figure S7a, Supporting Information). Furthermore the 149 nm DTMSPV-MSs was much more sensitive to Al^{3+} and Ru^{3+}, showing 17 and 54 times more sensitive to metal ions than the 270 nm size DTMSPV-πSs, respectively (Figure S7b, Supporting Information). Contrast to Al^{3+} and Ru^{3+}, the Cd^{2+} and Cu^{2+} showed almost similar quenching efficiency independent on the size of DTMSPV-NSs (Figure S7b, Supporting Information). This result indicates that metal ions such as Cd^{2+} and Cu^{2+}, which form static weak complexes with the surface sulfonate groups, should be less dependent on the size of DTMSPV-NSs.

Figure 7 summarizes schematically the formation of concentration dependent DTMSPV-NSs and their metal ion sensing. Al^{3+} forms plate structure through the interaction with triazine (**T**) units in DTMSPV. This Al^{3+} induced aggregations result in large quenching at 457 and 488 nm, broad emission spectrum,

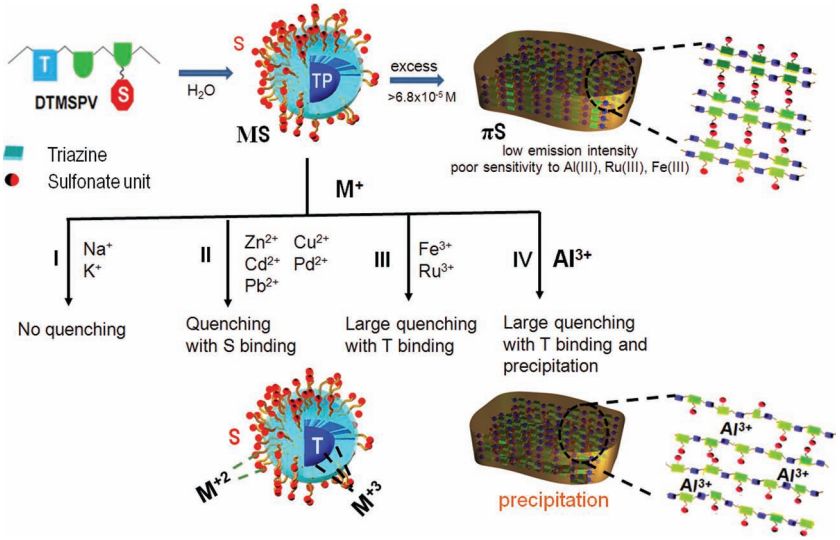

Figure 7. Schematic illustration for the formation of concentration dependent DTMSPV nanostructures and interaction between DTMSPV-MSs and metal ions.

and large red-shift in the fluorescence spectrum with maxima at 550 nm. The heavy quenching without spectral shift by Ru^{3+} and Fe^{3+} could be attributed to the interaction of these ions with triazine (**T**), which induces photo-induced electron transfer. The mechanism for the ion specific fluorescence quenching of conjugated polymers (P) containing SO_3^- groups has been described by the formation of static metal complex (P-SO_3^- + M^+ ↔ P-SO_3 M) that prevents electron transfer on the polymer or induces ultrafast photo-induced electron transfer to acceptor.[27,28] This static association of metal ions with polymer results in fluorescence quenching of conjugated polymers as the process for the recombination of excited electrons with holes to lead fluorescence is inaccessible. The predominant fluorescence quenching at the higher energy (457 nm) as well as small red-shifted emission in the presence of Pb^{2+}, Zn^{2+} or Cd^{2+} ion probably comes from the conformation change of DTMSPV-MSs in the close proximity of the ions, arising from the interaction of sulfonate (**S**) groups with metals.[29] It is likely that this ion recognition-induced conformation change does not contribute strongly to the lower energy emission (488 and 550 nm).

As the efficiency for the formation of the metal complex is highly dependent on the metal ions, the K_{sv} and the quenching efficiency (I_o/I) in in Table S1 (Supporting Information) stand for the metal type, charge, and outmost layer of electrons (OLC), in general, as similarly observed from other example of fluorescent conjugated polymers. Thus the quenching was larger in the order of the main group ions (I: Na^+, K^+) < dicationic transition metal ions (II, Zn^{2+}, Cd^{2+}, Pb^{2+} Cu^{2+}, Pd^{2+}) < trivalent transition metal ions (III, Fe^{3+}, Ru^{3+}), with an exception of Al^{3+}.

3. Conclusions

We synthesized a highly fluorescent polyelectrolyte (DTMSPV) with high fluorescence quantum yield (Φ_E) for selective detection of Al^{3+} from aqueous solutions. The DTMSPV with dual metal binding sites such as triazine and sulfonate units were

self-assembled into stable fluorescent nanostructures depending on DTMSPV concentration in aqueous solution. DTMSPV micelle like structures (DTMSPV-MSs) are sensitive to various metal ions, with the exception of alkali metals. The DTMSPV-MSs was exclusively sensitive to Al^{3+}, showing a color change from blue to yellow, resulting from the specific interaction of the triazine units of the polymer with Al^{3+}. Thus DTMSPV-MSs has excellent selectivity for Al^{3+}. Furthermore, Al^{3+} present in water was easily eliminated by filtration of precipitates formed by the complexation of the triazine units of the polymer and Al^{3+}. The metal ions could be categorized into two groups, triazine binding metals and sulfonate binding metals. Dications (Pb^{2+}, Zn^{2+}, Cd^{2+}, Cu^{2+}, and Pd^{2+}) mainly interact with sulfonate anions, while trivalent ions such as Fe^{3+} and Ru^{3} interact with the triazine units located inside MSs, not sulfonate anions. Al^{3+} forms plate structure through the interaction with triazine units in DTMSPV.

4. Experimental Section

Materials: Potassium *tert*-butoxide was purchased from TCI Co. (Japan) and used without purification. Other chemicals, solvents, and epoxy embedding medium kit were purchased from Aldrich and used as received. Poly(2-methoxy-5-propyloxy sulfonate, 1,4-phenylene vinylene (MPS-PPV), homopolymer without triazine unit as shown in Figure 1, was synthesized with Gilch polymerization according to previously reported procedures[30] for comparing the optical properties with DTMSPV.

Instruments and Sample Preparation: ^{1}H NMR spectra were obtained using a Varian Unity/Inova NMR 500 MHz spectrometer. FT–IR spectra were obtained using a TENSOR 37 (Bruker). UV spectra were obtained from a Guided Wave model 260 (Guided Wave, Inc., USA), and fluorescence spectra were obtained with a luminescence spectrometer (Perkin Elmer, Model LS55) under excitation at 370 nm. The absolute quantum yield of the water-soluble conjugated copolymer was determined using an absolute PL quantum yield measurement system (C9920-02, Hamamatsu Photonics, Shizuoka, Japan) at an excitation wavelength of 370 nm produced by a 150 W Xe lamp. The weight of DTMSPV and several metals was measured using a microbalance with an accuracy of 0.001 mg (Sartorius CPA2P, Germany). Polymer concentration was calculated with monomer repeat unit. The size distribution of DTMSPV nanoparticles were investigated by means of dynamic light scattering (DLS) in a ZEN 2001 (Malvern Instruments) and zeta potential measurements giving information about the stability of the suspensions were carried out using the same instrument. Scanning electron microscopy (SEM) images were obtained with a field-emission scanning electron microscope (FE-SEM) system (Hitachi, Model S-4200). Transmission electron microscopy (TEM) images were taken using at transmission electron microscope (JEM-2011(HC)) and a high-resolution transmission electron microscopy (HR-TEM) system (JEOL, Model JEM-3010). To prepare the samples for cross-sectional TEM images, DTMSPV solution was freshly dried, collected, and embedded in an epoxy resin made from dodecenylsuccinic anhydride, methyl nadic anhydride, 2,4,6-tris (dimethyl aminomethyl) phenol, and N-benzyldimethylamine in a 12:23:1:2 weight ratio and cured at 80 °C for 1 days. Thin sections for TEM were prepared using CR-X ultramicrotome (RMC Products) and a diamond knife operated in dry condition at room temperature. A cutting speed was 0.1 mm/s and a section thickness was approximately 70 nm. Micro-sections were deposited on the carbon coated TEM grids. For TEM measurements, the specimens were stained by exposing them to osmium tetroxide (OsO_4) vapor for 2 h. Since OsO_4 reacts preferentially with the unsaturated carbon double bonds of polymer backbone, the stained polymer backbone phase appears dark in a bright-field TEM micrograph.[31]

Synthesis of poly[(4,6-bis(formylphenoxy)-2-diphenylamino-s-triazine)-co(2-methoxy-5-propyloxysulfonate-1,4-phenylenevinylene)] (DTMSPV): 4, 6-bis (4-Formylphenoxy)-2-diphenyl amino-s-triazine (1) and 2-methoxy-5-(3-sulfonatopropoxy)-1,4-xylenebis(triphenylphosphoniumbromide) (2) were synthesized according to previously reported procedures with slight modifications, respectively (Figure 1).[32] Based on Wittig condensation, a 100 mL three-neck round bottom flask was charged with a mixture of anhydrous tert-butyl alcohol (4 mL), THF (12 mL), and DMF (12 mL). Compound 1 (0.30 g, 0.6 mmol) and compound 2 (0.57 g, 0.6 mmol) were added as solids. The mixture was then heated to 40 °C in an oil bath. Potassium tert-butoxide (0.35 g, 3.1 mmol) in anhydrous tert-butyl alcohol (5 mL) was added dropwise to the reaction solution from a dropping funnel for 5 min at 40 °C. The mixture was stirred for another 24 h after addition of the potassium tert-butoxide. The resulting polymer was precipitated out from methanol and collected by centrifugation. After drying under reduced pressure at room temperature, an orange solid DTMSPV (0.2 g) was obtained at an isolated yield percentage of 43%. ^{1}H NMR (DMSO), δ ppm: 6.95-7.65 (aromatic + vinylene), 4.45–5.10 (–O–CH_2–), 3.60–4.20 (–O–CH_3), 2.55–3.02 (–CH_2–SO_3), 1.20–2.20 (–CCH_2C–), FT–IR (cm^{-1}): 1600 (C=N), 1500 (C–N), 865 (cis-vinylene) (Figure S1, Supporting Information). M_n (NMR) = 13 200.

Determination of the average molar mass of DTMSPV using gel permeation chromatography (GPC, Waters Model 515 pump, Waters Model 2410 differential refractometer, and Waters 996 photodiode array detector using PLaquagel-OH30 and TSKgel G2500+G4000 columns) was hampered, most likely because of the strong adsorption of DTMSPV to the column.[33] The GPC approach also has the intrinsic limitation of a lack of suitable calibration standards. Therefore, NMR spectroscopy was used to determine average molar mass (M_n) for DTMSPV with defined end groups of aldehyde.

Supporting Information

Supporting Information is available from the Wiley Online Library or from the author.

Acknowledgements

We acknowledge the financial support of a Ministry of Knowledge Economy (MKE), National Research Foundation (NRF) grant funded by the Korean government (MEST) through the Active Polymer Center for Pattern Integration (APCPI) (R11-2007-050-00000-0), the Pioneer Research Center Program through the National Research Foundation of Korea funded by the Ministry of Education, Science and Technology (2011-0001672), and Converging Research Center Program through the Ministry of Education, Science and Technology (2011K000631).

Received: September 27, 2011
Published online: February 2, 2012

[1] a) K. Ariga, A. Vinu, Q. Ji, O. Ohmori, J. P. Hill, S. Acharya, J. Koike, S. Shiratori, *Angew. Chem. Int. Ed.* **2008**, *47*, 7254; b) Q. Ji, S. B. Yoon, J. P. Hill, A. Vinu, J.-S. Yu, K. Ariga, K. Ariga, *J. Am. Chem. Soc.* **2009**, *131*, 4220; c) Q. Ji, I. Honma, S.-M. Paek, M. Akada, J. P. Hill, A. Vinu, K. Ariga, *Angew. Chem. Int. Ed.* **2010**, *49*, 9737; d) T. Mori, K. Okamoto, H. Endo, J. P. Hill, S. Shinoda, M. Matsukura, H. Tsukube, Y. Suzuki, Y. Kanekiyo, K. Ariga, *J. Am. Chem. Soc.* **2010**, *132*, 12868; e) T. Michinobu, S. Shinoda, T. Nakanishi, J. P. Hill, K. Fujii, T. N. Player, H. Tsukube, K. Ariga, *Phys. Chem. Chem. Phys.* **2011**, *13*, 4895.

[2] a) N. Song, H. Zhu, Sh. Jin, W. Zhan, T. Lian, *ACS Nano* **2011**, *5*, 613; b) T. Zhang, J. L. Stilwell, D. Gerion, L. Ding, O. Elboudwarej, P. A. Cooke, J. W. Gray, A. P. Alivisatos, F. F. Chen, *Nano Lett.* **2006**, *6*, 800.

[3] K. E. Sapsford, L. Berti, I. L. Medintz, *Angew. Chem. Int. Ed.* **2006**, *45*, 4562.

[4] a) C.-C. You, O. R. Miranda, B. Gider, P. S. Ghosh, I.-B. Kim, B. Erdogan, S. A. Krovi, U. H. F. Bunz, V. M. Rotello, *Nat. Nanotechnol.* **2007**, *2*, 318; b) O. R. Miranda, C.-C. You, R. Phillips,

I.-B. Kim, P. S. Ghosh, U. H. F. Bunz, V. M. Rotello, *J. Am. Chem. Soc.* **2007**, *129*, 9856.
[5] a) H. Zhu, M. J. McShane, *J. Am. Chem. Soc.* **2005**, *127*, 13448; b) H. Wang, W. You, P. Jiang, L. Yu, H. H. Wang, *Chem. Eur. J.* **2004**, *10*, 986; c) S. Lin, Y. Tung, W. Chen, *J. Mater. Chem.* **2008**, *18*, 3985.
[6] a) F. Gouanvé, T. Schuster, E. Allard, R. Méallet-Renault, C. Larpent, *Adv. Funct. Mater.* **2007**, *17*, 2746; b) H. Goesmann, C. Feldmann, *Angew. Chem. Int. Ed.* **2010**, *49*, 1362.
[7] a) A. Burns, P. Sengupta, T. Zedayko, B. Baird, U. Wiesner, *Small* **2006**, *2*, 723; b) J. Ji, N. Rosenzweig, C. Griffin, Z. Rosenzweig, *Anal. Chem.* **2000**, *72*, 3497; c) J. M. Kürner, O. S. Wolfbeis, I. Klimant, *Anal. Chem.* **2002**, *74*, 2151; d) A. Mallick, M. C. Mandal, B. Haldar, A. Chakrabarty, P. Das, N. Chattopadhyay, *J. Am. Chem. Soc.* **2006**, *128*, 3126.
[8] a) C. Tan, E. Atas, J. G. Müller, M. R. Pinto, V. D. Kleiman, K. S. Schanze, *J. Am. Chem. Soc.* **2004**, *126*, 13685; b) C.-C. Wang, H. Tsai, H.-H. Shih, S. Jeon, Z. Xu, D. Williams, S. Iyer, T. C. Sanchez, L. Wang, M. Cotlet, H.-L. Wang, *ACS Appl. Mater. Interfaces* **2010**, *2*, 738; c) M. Vetrichelvan, L. Hairong, R. Ravindranath, S. Valiyaveetil, *J. Polym. Sci. Pol. Chem.* **2006**, *44*, 3763; d) A. N. Kuskov, M. I. Shtilman, A. V. Goryachaya, R. I. Tashmuhamedov, A. A. Yaroslavov, V. P. Torchilin, A. M. Tsatsakis, A. K. Rizos, *J. Non-cryst. Solids* **2007**, *353*, 3969.
[9] S. M. Thomas III, G. D. Joly, T. M. Swager, *Chem. Rev*. **2007**, *107*, 1339.
[10] G. Ramachandran, T. A. Smith, D. Gómez, K. P. Ghiggino, *Synth. Met.* **2005**, *152*, 17.
[11] C. Metcalfe, C. Rajput, J. A. Thomas, *J. Inorg. Biochem.* **2006**, *100*, 1314.
[12] D. Sun, S. Ma, Y. Ke, T. M. Petersen, H.-C. Zhou, *Chem. Commun.* **2005**, 2663.
[13] E. I. Lerner, S. J. Lippard, *J. Am. Chem. Soc.* **1976**, *98*, 5397–5398.
[14] N. Umezawa, R. K. Kalia, A. Nakano, P. Vashista, F. Shimojo, *J. Chem. Phys.* **2007**, *126*, 234702–1.
[15] a) J. Yoo, T. Kwon, B. D. Sarwade, Y. Kim, E. Kim, *APPL. PHYS. LETT.* **2007**, *91*, 241107–1; b) J. You, J. S. Heo, J. Lee, H.-S. Kim, H. O. Kim, E. Kim, *Macromolecules.* **2009**, *42*, 3326.
[16] C. Tan, M. R. Pinto, E. Kose, I. Ghiviriga, K. S. Schanze, *Adv. Mater.* **2004**, *16*, 1208.
[17] a) L. Cheng, G. Hou, J. Miao, D. Chen, M. Jiang, L. Zhu, *Macromolecules* **2008**, *41*, 8159; b) A. Walther, M. Drechsler, S. Rosenfeldt, L. Harnau, M. Ballauff, V. Abetz, A. H. E. Mller, *J. Am. Chem. Soc.* **2009**, *131*, 4720.
[18] A. Kumar, S. K. Menon, *Eur. J. Med. Chem.* **2009**, *44*, 2178.
[19] S. Deshmukh, L. Bromberg, K. A. Smith, T. A. Hatton, *Langmuir* **2009**, *25*, 3459.
[20] a) J. Kim, T. M. Swager, *Nature* **2001**, *411*, 1030; b) D. T. McQuade, J. Kim, T. M. Swager, *J. Am. Chem. Soc.* **2000**, *122*, 5885.
[21] a) C. Tan, M. R. Pinto, K. S. Schanze, *Chem. Commun.* **2002**, *5*, 446; b) N. DiCesare, M. R. Pinto, K. S. Schanze, J. R. Lakowicz, *Langmuir* **2002**, *18*, 7785.
[22] a) D.-H. Hwang, J.-I. Lee, N.-S. Cho, H.-K. Shim, *J. Mater. Chem.* **2004**, *14*, 1026; b) R. M. Gurge, A. M. Sarker, P. M. Lahti, B. Hu, F. E. Karasz, *Macromolecules*, **1997**, *30*, 8286; c) P. Piatkowski, W. Gadomski, P. Przybylski, B. Ratajska-Gadomska, *J. Photochem. Photobiol. A* **2010**, *215*, 69; d) Y.-H. Kim, H.-O. Lee, S.-O. Jung, S.-K. Kwon, *Macromol. Res.* **2003**, *11*, 194–197.
[23] J. S. Treger, V. Y. Ma, Y. Gao, C.-C. Wang, H.-L. Wang, M. S. Johal, *J. Phys. Chem. B* **2008**, *112*, 760.
[24] Z. Hashim, P. Howes, M. Green, *J. Mater. Chem.* **2011**, *21*, 1797.
[25] a) H. Tong, L. Wang, X. Jing, F. Wang, *Macromolecules* **2002**, *35*, 7169; b) D. Shen, L. Wang, Z. Pan, S. Cheng, X. Zhu, L.-J. Fan, *Macromolecules* **2011**, *44*, 1009; c) J. Kim, D. T. McQuade, S. K. McHugh, T. M. Swager, *Angew. Chem. Int. Ed.* **2000**, *39*, 3868.
[26] a) T. D. Gauthier, E. C. Sham, W. F. Guerln, W. R. Seltz, C. L. Grant, *Environ. Sci. Technol.* **1986**, *20*, 1162; b) W. Wang, W. Min, J. Chen, X. Wu, Z. Hu, *J. Lumin.* **2011**, *131*, 820.
[27] Y.-G. Chen, D. Zhao, Z.-K. He, X.-P. Ai, *Spectrochimica Acta Part A* **2007**, *66*, 448.
[28] H. Liu, S. Wang, Y. Luo, W. Tang, G. Yu, L. Li, C. Chen, Y. Liu, F. Xi, *J. Mater. Chem.* **2001**, *11*, 3063.
[29] Z. Chen, C. Xue, W. Shi, F.-T. Luo, S. Green, J. Chen, H. Liu, *Anal. Chem.* **2004**, *76*, 6513.
[30] a) A. D. Smith, C. K.-F. Shen, S. T. Roberts, R. Helgeson, B. J. Schwartz, *Res. Chem. Intermed.* **2007**, *33*, 125; b) J. Dalvi-Malhotra, L. Chen, *J. Phys. Chem. B* **2005**, *109*, 3873.
[31] Y. Oeda, O. Nishi, Y. Matsushima, K. Mizuno, A. H. Matsui, M. Michinomae, M. Takeshima, T. Goto, *Chem. Phys.* **1996**, *213*, 421.
[32] Z. Gu, Y.-J. Bao, Y. Zhang, M. Wang, Q.-D. Shen, *Macromolecules* **2006**, *39*, 3125.
[33] S. Kim, J. Jackiw, E. Robinson, K. S. Schanze, J. R. Reynolds, *Macromolecules* **1998**, *31*, 964.